Journal of Nuclear Materials 383 (2009) 215–225

Contents lists available at ScienceDirect

Journal of Nuclear Materials

journal homepage: www.elsevier.com/locate/jnucmat

Effect of heating and cooling rate on the kinetics of allotropic phase changes in uranium: A differential scanning calorimetry study

Arun Kumar Rai [a], S. Raju [a,*], B. Jeyaganesh [a], E. Mohandas [a], R. Sudha [b], V. Ganesan [b]

[a] Physical Metallurgy Division, Indira Gandhi Centre for Atomic Research (IGCAR), Kalpakkam 603 102, Tamilnadu, India
[b] Materials Chemistry Division, Indira Gandhi Centre for Atomic Research (IGCAR), Kalpakkam 603 102, Tamilnadu, India

ARTICLE INFO

Article history:
Received 14 July 2008
Accepted 11 September 2008

ABSTRACT

The kinetic aspects of allotropic phase changes in uranium are studied as a function of heating/cooling rate in the range 10^0–10^2 K min^{-1} by isochronal differential scanning calorimetry. The transformation arrest temperatures revealed a remarkable degree of sensitivity to variations of heating and cooling rate, and this is especially more so for the transformation finish (T_f) temperatures. The results obtained for the $\alpha \rightarrow \beta$ and $\beta \rightarrow \gamma$ transformations during heating confirm to the standard Kolmogorov–Johnson–Mehl–Avrami (KJMA) model for a nucleation and growth mediated process. The apparent activation energy Q_{eff} for the overall transformation showed a mild increase with increasing heating rate. In fact, the heating rate normalised Arrhenius rate constant, k/β reveals a smooth power law decay with increasing heating rate (β). For the $\alpha \rightarrow \beta$ phase change, the observed DSC peak profile for slower heating rates contained a distinct shoulder like feature, which however is absent in the corresponding profiles found for higher heating rates. The kinetics of $\gamma \rightarrow \beta$ phase change on the other hand, is best described by the two-parameter Koistinen–Marburger empirical relation for the martensitic transformation.

1. Introduction

Uranium exists in three allotropic modifications, namely α-orthorhombic, β-tetragonal and γ-bcc, in the order of increasing temperature [1]. Owing to the fact that uranium being a reactive metal and is prone to easy oxidation and picking up of impurities, a certain scatter is found among the reported values for the transformation temperatures in literature [2–6]. In his supplementary assessment of U–Zr phase diagram, Okamoto recommends, 941 K (668 °C) and 1049 K (776 °C), respectively for $\alpha \Leftrightarrow \beta$ and $\beta \Leftrightarrow \gamma$ transformations [7]. The allotropic phase changes in pure uranium have attracted a great deal of interest right from the early days of research on actinide metallurgy [8–18]. Thus for example, it has been established that both $\gamma \rightarrow \beta$ and $\beta \rightarrow \alpha$ transformation temperatures are very sensitive to the cooling rate from the high temperature γ-bcc phase [15]. A highly non-linear decrease in the transformation temperatures with increasing rate of cooling in the range, 10^0 to 10^4 K s^{-1} has been found [15]. A similar scenario is witnessed during heating for the $\alpha \rightarrow \beta$ transformation as well for a smaller range of heating rate variation [2]. These early studies clearly revealed that it is rather difficult to quench-retain the intermediate β phase in pure uranium at room temperature, since the $\beta \rightarrow \alpha$ transformation kinetics is very rapid and it becomes necessary to alloy uranium with small amounts of transition element to stabilise the β phase at room temperature [8]. It has been convincingly argued by Burke [16] following a critical appraisal of the experimental findings available then [8–15], that the $\beta \rightarrow \alpha$ structural change can assume different mechanisms under different cooling rate regimes. In fact, a TTT curve with two noses that are separated by a plateau is postulated for the formation of α from β [9,16]. It must be added that there exists an extensive literature on the physical metallurgy of uranium alloys covering thermodynamic, structural and phase transformation aspects (see Ref. [1,8]). Nevertheless, many issues related to the fundamental kinetic aspects of these phase changes still remain unclear [8,17,18]. A comprehensive account of the intricacies of the $\alpha \Leftrightarrow \beta$ phase transformation in uranium is provided by Vandermeer, who used dilatometry and metallography to monitor the β formation kinetics [18]. This study supported the possibility of massive $\beta \rightarrow \alpha$ phase change, and using light microscopy measurements and Turnbull's theory of interface controlled phase transformation [19], an estimate of the average velocity of the transformation front has also been estimated. Subsequent to Vandermeer's study not much progress has been made in explaining the basic issues of various phase transformations in uranium and uranium alloys. Subsequent to this study, to the best of our knowledge, we are not aware of any controlled thermal analysis investigation of the transformation kinetics at the lower end of the heating and cooling rate spectrum in the recent past. One of the aims of this investigation is to fill in this gap.

With the recent advances in physical metallurgy, both on conceptual and experimental fronts, the study of transformation

* Corresponding author. Tel.: +91 44 274 80 306; fax: +91 44 274 80 081.
E-mail address: sraju@igcar.gov.in (S. Raju).

0022-3115/$ - see front matter © 2008 Elsevier B.V. All rights reserved.
doi:10.1016/j.jnucmat.2008.09.012

kinetics, especially, its finer aspects with respect to bulk diffusive and interface controlled phase transformations have received an increased attention in the recent past [20–24]. In the light of such a scenario, it is rather stimulating to reinvestigate the phase transformations in uranium alloys from the point of view of fostering a broad based understanding of transformation kinetics.

A study on uranium is also of interest on applied grounds as well. With the revival of interest in metal-fuelled fast reactors, the knowledge of physical metallurgical aspects associated with developing uranium based metallic fuels assumes special significance in realising the optimal choice of fuel composition. Since any uranium alloy that is present inside the core as a fast reactor fuel is bound to experience numerous thermal transients and hence phase change cycles, it is useful to investigate the kinetics of temperature driven structural phase changes in potential uranium based metallic fuel alloys. As a part of such research program, it is decided to investigate the role of heating and cooling rates on the structural changes in pure uranium itself, since a clear enunciation of relevant issues in a relatively simple system as pure uranium, is vital to evolving a proper appreciation of composition mediated effects, which are likely to be encountered in uranium based multi component alloys. The experimental technique adopted for this purpose is thermal analysis in the form of differential scanning calorimetry (DSC). The details of the experiments are briefly listed below.

2. Experimental procedure

The unenriched natural uranium metal used in this study is obtained in the form of cylindrical, vacuum induction melted and cast rods of about 5 mm in diameter. The chemical composition is listed in Table 1. Carbon (316 wt.ppm), oxygen (552 wt.ppm) and nitrogen (241 wt.ppm) happen to be the major impurities in the uranium used in this study. From the rod, a few thin slices are precision cut using diamond coated wire saw under slow speeds. These are further polished by fine emery for ensuring smooth surface finish and are ultrasonically cleaned in pure acetone. The samples for metallography were prepared using standard methods and were observed in a scanning electron microscope (Philips XL 30®) immediately after diamond polishing in the unetched condition, since pure uranium tends to get tarnished rather quickly. In Fig. 1(a), the typical scanning electron micrograph of the uranium sample in the unetched condition is illustrated. As can be seen, the grain size of the starting microstructure is rather large and is estimated to be in the range 350–400 μm. The necklace like decoration of the α phase grain boundary is due to coarse uranium silicide particles which are identified using EDX spectra shown in Fig. 1(b). The samples for DSC studies are obtained in the form of small cubes of about 1.5 mm in length and of mass that varied generally between 30 and 50 ± 0.01 mg. A commercial high temperature heat-flux DSC (Setaram setsys evolution 1600 with type S thermocouple) is used for imposing controlled heating and cooling schedules. The specimen is housed in a well cleaned 100 μL cylindrical recrystallised alumina crucible inside the DSC cradle, which is alternately evacuated and purged with high purity argon (Iolar grade I; oxygen ≈ 0, moisture <2 ppm, nitrogen <2 ppm) a few times, before the commencement of an experimental run. A steady flow of argon of about 50 ml per minute is maintained through out the experiment. Although argon being a poor conductor of heat, as compared to say, helium, the constant and steady trickle of argon served to minimise the thermal turbulence through out the experiment and this is necessary in ensuring wiggle free base-line runs, as argon in this case is a sink for heat. Since the mass of our samples including pure metal references are in mill gram range, it is believed that the use of argon in place of a better heat conductor like helium will not seriously skew the caloric calibration of the signal [25]. It is found in case of pure iron, which is used also used as a secondary calibrant, that for slow heating and cooling rate scans (1 K min^{-1}), there will not be any appreciable temperature gradient across the section thickness of the DSC sample. This is judged by the sharpness of the transformation peak and also from the absence of multiple serrations arising from discrete melting events. The issues involved in DSC calibration is discussed by Richardson [25] and in deference to brevity, these aspects are not dealt

Table 1
The chemical composition of the uranium sample as determined using ICP-AES

Al	Cd	Ce	Co	Cr	Dy	Er	Eu	Fe	Gd	Mg	Mn	Ni	Sm	Y	Yb	C	N	O	Si
349	<0.12	2.2	0.2	14.7	<0.1	<0.1	<0.04	73.5	0.04	11.1	9.3	32.5	0.4	<0.1	<0.1	316	241	552	615

The quoted figures are in weight ppm basis.

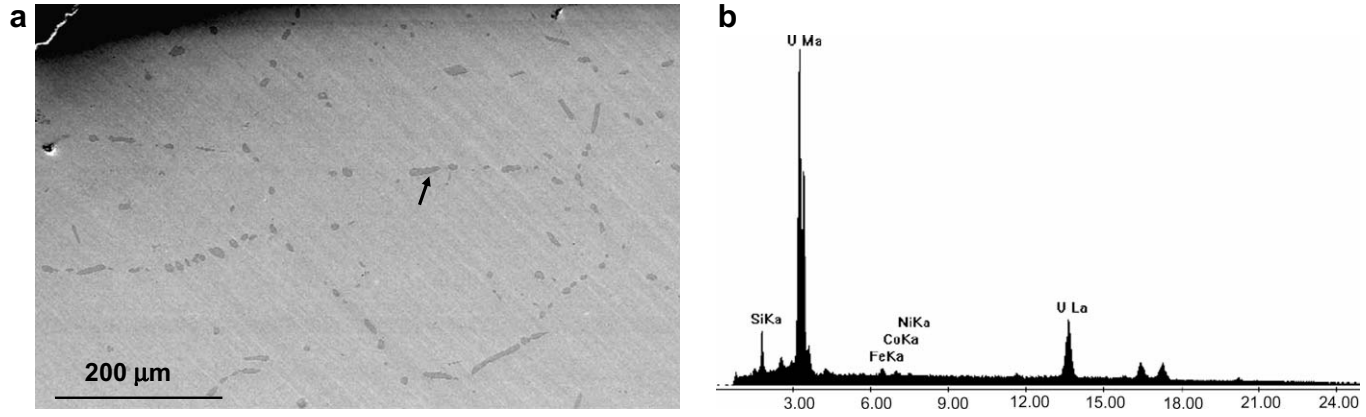

Fig. 1. (a and b) The scanning electron micrograph of the starting microstructure of the uranium sample used in the present study. The arrow denotes a typical intergranular uranium silicide particle. (b) EDX spectrum from the particle shown by arrow.

with in detail here. A typical isochronal DSC run employed in the present study consists of following heating and cooling schedules:

(i) To begin with, the furnace temperature is gradually raised to 473 K (200 °C) and is allowed to stabilise at this temperature for about 15 min. This is required for the attainment of thermal equilibrium of the system before starting any measurement. Such preconditioning also facilitates the attainment of a smooth non-wavy base-line. This step is followed by actual heating ramps and holding isotherms that are characteristic of present DSC experiments.

(ii) In an actual experimental run, the sample is heated at a pre determined rate from 473 (200 °C) to 1323 K (1050 °C) and is equilibrated at this temperature for about 15 minutes, and then cooled at the same scan rate to 473 K, again kept at this temperature for a period of about 15 min, before cooling to room temperature. The scanning rate employed is varied between 1 and 100 K min^{-1}. Fresh samples are employed for each individual run and a few repeat runs are also performed for select heating rates (10 and 99 K min^{-1}) in order to assess the reproducibility at either end of the scan rate spectrum.

(iii) The base-line calibration runs have been performed for each heating rate under identical experimental heating and cooling conditions using the *same* pair of empty crucibles on both sides of the DSC specimen cradle. The temperature calibration has been done using the melting points of pure aluminium, zinc, tin, copper, silver, gold, and iron (80 ppm carbon: Aldrich) standards. The heat flow calibration around the region of phase transformation is done in terms of the known C_p change of the $\alpha \rightarrow \gamma$ transformation in pure iron. In addition, the melting transitions in gold, silver and copper have also been used for supplementing the enthalpy calibration. The temperature accuracy in case of low heating rate experiments (1–30 K min^{-1}) is found to be ±2 K for samples of mass up to 50–100 mg; while, it is little poorer, of the order of ±4 K for high heating rates (99 K min^{-1}). The degree of reproducibility of repeat runs is found to be ±1 K. Since reliable and reproducible temperature and heat flow calibration of a DSC during cooling cycle is comparatively a difficult proposition [25–28], the calibration of the signal was carried out only for the heating cycle in the present study. It is presumed that this is approximately valid for the cooling cycle as well.

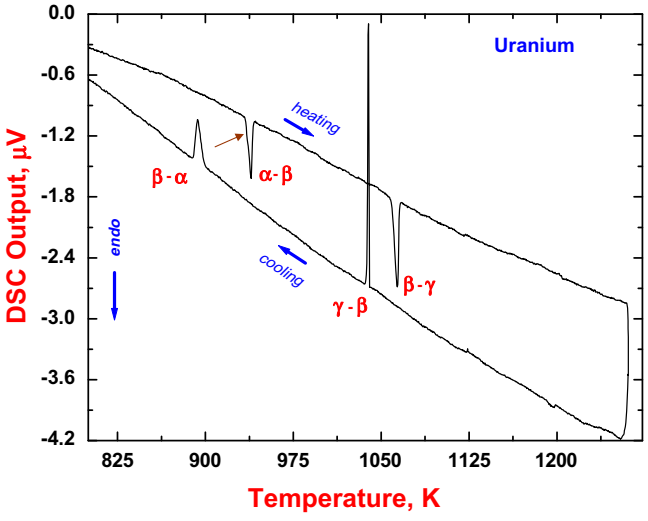

Fig. 2. A typical DSC profile illustrating the transformation peaks associated with the polymorphic phase changes in uranium.

3. Results

3.1. Transformation peak profiles and transformation temperatures

In Fig. 2, a typical DSC profile obtained during a 3 K min^{-1} heating and cooling schedule is displayed. Very sharp transformation peaks associated with the heat effects of $\alpha \Leftrightarrow \beta$ and $\beta \Leftrightarrow \gamma$ transformations are clearly revealed. A considerable degree of under cooling is also noticed for both $\gamma \rightarrow \beta$ and $\beta \rightarrow \alpha$ transformations. Further, a careful inspection of the $\alpha \rightarrow \beta$ endothermic transformation peak indicates the presence of a very weakly discernible shoulder like feature, which is marked by arrow. This is more clearly brought out in Fig. 3(a), wherein the $\alpha \rightarrow \beta$ peak profiles observed for smaller heating rates (1–30 K min^{-1}) are collated together. In order to enhance clarity, we have sketched only the transformation profile zone using the no sample base-line subtracted DSC profiles and this base-line compensation is done for each scan rate independently. Since the present study focuses on the transformation kinetics, the mapping of the ordinate of DSC plot in terms of heat flow rate is not done here; its calibration into J/g, K basis is however done during Cp measurements, which is not reported here. A clear shoulder like feature is noticed for 1, 3, and 5 K min^{-1} heating rate scans. In fact, this shoulder is fairly resolved only for very low heating rate scans, and is found to gradually merge with the main part of the peak profile as the heating rate is increased (*compare*, Fig. 3(a) and (b)). A similar set of transformation peak profiles are obtained for the $\beta \rightarrow \gamma$ phase change as well; but with the difference that no specific shoulder like splitting is seen in this case for low heating rate scans. The individual peak profiles are not presented here in order to avoid unnecessary proliferation of graphical information. In Fig. 4, the heating or cooling rate (β) induced variations of transformation start (T_s), peak (T_p) and finish temperatures (T_f) for both $\alpha \Leftrightarrow \beta$ and $\beta \Leftrightarrow \gamma$ transformations are graphically illustrated.

Although a general increase (decrease) of the transformation temperatures to varying extents with heating (cooling) rate is clearly revealed in Fig. 4, it is nevertheless interesting to note that this increase is highly non-linear in nature. This non-linear behaviour is quite remarkably revealed in the heating rate variation of T_f, the transformation finish temperature. On the contrary, the T_s temperature after a clear initial increase at the slow heating rate regime (2–7 K min^{-1}) evinces a sort of plateau for higher values of β. As a result, the width of the transformation domain given by the temperature interval T_f–T_s, increases effectively with increasing heating rate, implying thereby a kinetics induced expansion of ($\alpha + \beta$) and ($\beta + \gamma$) two phase fields at higher heating rates. The transformation temperatures for both $\alpha \rightarrow \beta$ and $\beta \rightarrow \gamma$ structural changes measured for the slowest heating rate of 1 K min^{-1} recorded in the present work are 936 ± 2 K (663 °C) and 1056 ± 2 K (783 °C), respectively. Notwithstanding the presence of impurities in our starting material (Table 1) and the invariable presence of thermal lag in the DSC equipment (the influence of this factor has been minimised by proper temperature calibration; but not altogether eliminated), these values are fairly in agreement with the ones quoted in the literature for the equilibrium transformation temperature [1,2]. In Table 2, the experimentally measured heating rate variations of transformation temperatures and peak areas are listed. One final point to note in Fig. 4, is that for the $\beta \rightarrow \alpha$ phase change, the observed T_s value for 99 K min^{-1} seems to be somewhat higher, which is contrary to the expected decreasing trend. Since in the present study, higher than 100 K min^{-1} cooling could not be achieved, it could not be ascertained by higher cooling rate experiments as to whether this upheaval represents a genuine physical effect like the onset of a new plateau, or is it arising from the unavoidable experimental scatter.

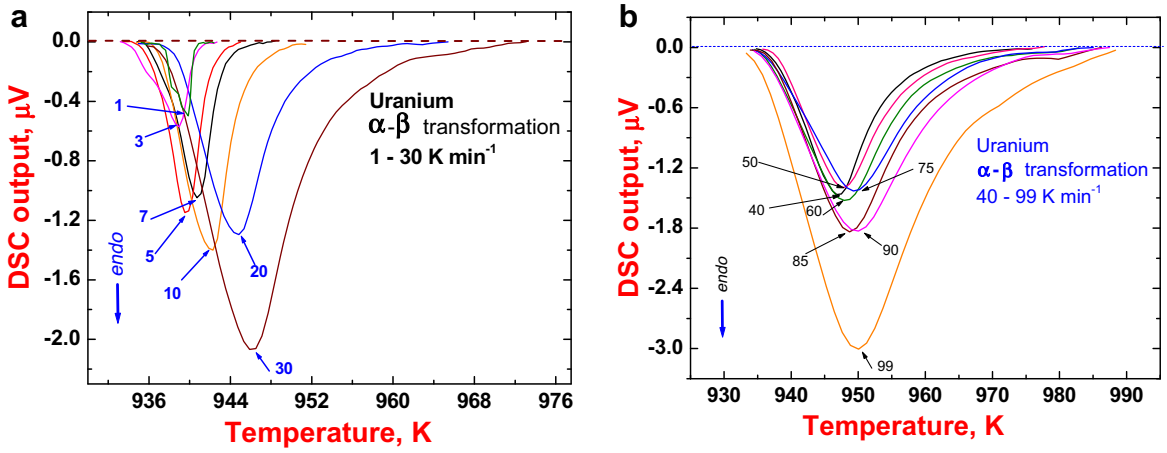

Fig. 3. (a) The DSC profiles for the α → β transformation obtained at lower heating rates are stacked together. The occurrence of shoulder like feature for slow heating scans is readily seen. (b) Gives the same data for higher heating rates.

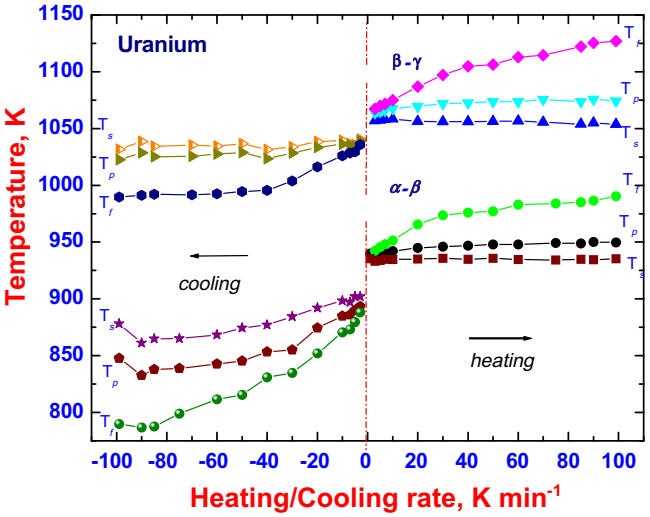

Fig. 4. A graphical portrayal of the non-linear variation of the transformation start (T_s), peak (T_p) and finish (T_f) temperatures with heating/cooling rate. For the β → α phase change, the observed T_S value for 99 K min^{-1} seems to be somewhat higher, which is contrary to the expected decreasing trend. Since in the present study, higher than 100 K min^{-1} cooling could not be achieved, it could not be ascertained, whether this represents a genuine physical effect like the onset of a new plateau, or is it arising from the experimental scatter.

In Figs. 5(a) and (b) the DSC peak profiles of γ → β and β → α transformations that occur during the cooling part of thermal cycle are illustrated. Again, for the sake of brevity, only the low heating rate traces are presented. As a general remark, it may be added that the γ → β peak profiles are fairly sharp and smooth for the entire range of cooling rate adopted in this study; on the contrary, the β → α profiles contained some undulations for slow heating rates (see, the circled region in 1 K min^{-1} scan in Fig. 5(b)). The cooling rate dependencies of respective transformation temperatures are illustrated in the left half of the composite Fig. 4. Again the non-linear variation of the transformation temperatures with respect to cooling rate is readily apparent. For a cooling rate of 1 K min^{-1}, the observed transformation start (T_s) temperatures for γ → β and β → α transformations are 1038 K (765 °C) and 913 K (640 °C), respectively. In Table 3, the experimentally measured cooling rate variations of γ → β and β → α transformation arrest temperatures are listed.

3.2. Transformation plots

From the experimental DSC peak profile, the fractional extent of transformation as a function of temperature $X(T)$, is estimated using the following expression

$$X(T) = \left\{ \left(\int_{T_s}^{T} \phi(T)\mathrm{d}T \right) / \left(\int_{T_s}^{T_f} \phi(T)\mathrm{d}T \right) \right\}. \quad (1)$$

Here, the integral in the numerator, namely, ${}_{T_s}\int^{T}\phi(T)\mathrm{d}T$, stands for the partial area under the peak in the temperature domain T_s–T. The denominator ${}_{T_s}\int^{T_f}\phi(T)\mathrm{d}T)$ stands for the total peak area covering the entire transformation temperature range (T_s–T_f). Eq. (1) assumes that transformation is complete upon reaching T_f, although this is certainly not true for higher heating rates. The transformation plots obtained using Eq. (1) are displayed in Fig. 6(a) for α → β, and in (b) for β → γ, respectively. In Figs. 7(a) and (b), these are presented for γ → β and β → α transformations respectively.

3.3. Empirical description of transformation kinetics

As had been briefly sketched in the introduction, both nucleation and growth and martensitic modes of transformations are found in uranium. In the classical methodology adopted for analysing the kinetics of a nucleation and growth type of transformation as studied by thermal analysis methods, the following separable functional representation is often invoked to represent the instantaneous reaction rate, $(\partial X/\partial t)_\beta$ [29]

$$(\partial \mathrm{X}/\partial t)_\beta = (\partial \mathrm{X}/\partial \mathrm{T})_\beta \times \beta = \mathrm{f(X)k(T)}. \quad (2)$$

In the above expression, $f(X)$ is often taken to be an empirical, but suitable reaction model that is consistent with the established kinetic features of the transformation under consideration. The empirical rate constant $k(T)$ is normally assumed to be of the Arrhenius form

$$k = k_0 \exp(-Q_{\mathrm{eff}}/RT), \quad (3)$$

with Q_{eff} being the *effective* or *apparent* activation energy for the *overall* transformation process. In general terms, Q_{eff} must be treated as dependent on the transformation extent $X(T)$ as well, but for reasons of convenience and simplicity, is often taken to be a constant. A few technical points need be elaborated with regard to the application of Eq. (2) in explaining the non-isothermal reaction kinetics.

It is a standard practice to use Eq. (2) in conjunction with the additivity rule for explaining the transformation kinetics occurring

Table 2
Listing of the α → β and β → γ transformation arrest temperatures and associated peak areas as a function of heating rate for pure uranium

Heating rate (K min^{-1})	T_s α → β (K)	T_p α → β (K)	T_f α → β (K)	Peak area α → β (μV s/mg)	T_s β → γ (K)	T_p β → γ (K)	T_f β → γ (K)	Peak area β → γ (μV s/mg)
1	935.2	939.9	942.1	1.57	1055.6	1064.5	1067.2	2.35
3	933.2	939.0	942.4	1.61	1057.0	1063.9	1067.3	2.59
5	933.9	939.6	945.5	1.59	1057.2	1065.3	1070.0	2.51
7	934.9	940.8	948.1	1.64	1058.1	1066.1	1071.8	2.66
10	934.8	942.0	951.5	1.39	1058.4	1067.7	1075.1	2.21
20	935.2	944.9	965.5	1.53	1056.3	1069.5	1087.0	2.45
30	935.9	946.0	973.6	1.48	1056.0	1071.9	1097.3	2.46
40	934.9	946.9	976.0	1.37	1056.0	1072.6	1104.9	2.44
50	935.8	948.0	977.1	1.34	1056.2	1073.6	1106.4	2.35
60	934.6	948.0	982.9	1.28	1056.7	1073.6	1112.9	2.27
75	934.3	949.3	984.1	1.11	1055.7	1075.5	1114.5	2.16
85	934.7	948.8	985.2	1.30	1054.0	1073.6	1122.2	2.60
90	934.5	950.1	986.4	1.20	1055.0	1075.9	1125.4	2.22
99	933.3	950.0	988.4	1.18	1054.3	1076.1	1126.3	2.27

The temperatures are rounded of to one decimal point, while the peak areas to two decimal points.

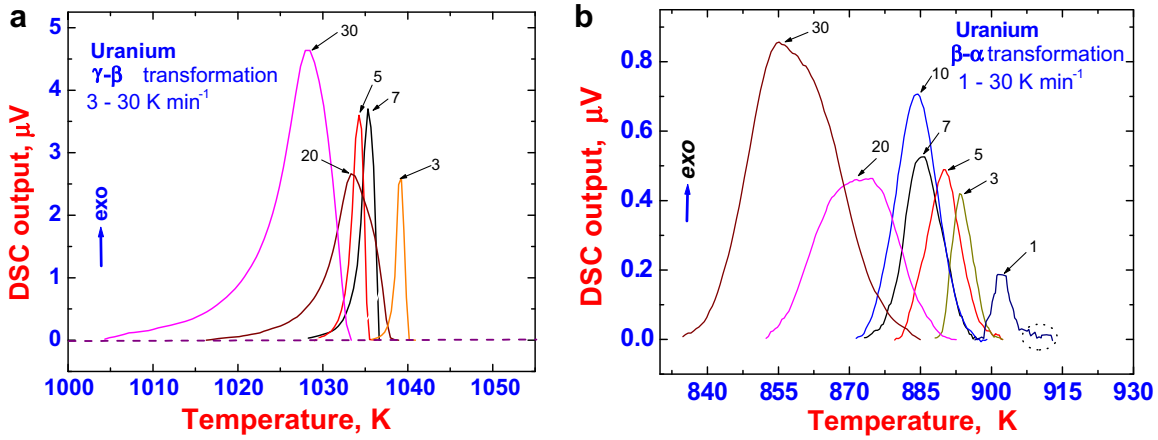

Fig. 5. (a) DSC profiles for the γ → β transformation during cooling. (b) DSC profiles for the β → α transformation during cooling.

Table 3
Listing of the γ → β and β → α transformation temperatures and the associated peak area as a function of cooling rate for pure uranium

Cooling rate (K min^{-1})	T_s γ → β (K)	T_p γ → β (K)	T_f γ → β (K)	Peak area γ → β (μV s/mg)	T_s β → α (K)	T_p β → α (K)	T_f β → α (K)	Peak area β → α (μV s/mg)
1	1038.8	1038.7	1037.2	2.70	912.9	901.3	897.9	1.71
3	1040.6	1039.3	1035.8	2.70	902.0	893.3	888.2	1.74
5	1035.9	1034.3	1029.5	2.61	902.1	889.9	879.6	1.78
7	1036.7	1035.4	1028.4	2.79	897.0	886.0	873.2	1.83
10	1039.5	1036.3	1026.0	2.35	898.3	884.9	870.6	1.55
20	1038.5	1033.4	1016.3	2.61	892.1	874.5	852.0	1.68
30	1033.7	1028.5	1003.8	2.63	884.5	855.2	834.9	1.57
40	1031.5	1023.5	995.7	2.54	877.1	853.4	830.9	1.38
50	1036.8	1029.0	994.6	2.62	874.5	845.4	815.4	1.26
60	1034.5	1027.6	992.6	2.35	868.4	842.8	811.5	1.49
75	1035.5	1025.7	991.7	2.29	865.0	838.7	798.9	1.77
85	1034.3	1025.1	992.2	2.81	864.9	838.0	787.7	1.86
90	1038.7	1028.7	991.2	2.60	861.1	832.6	786.7	2.04
99	1031.7	1022.6	989.7	2.79	878.1	847.6	789.9	2.66

during continuous heating or cooling [30]. It must be admitted however, that in a rigorous sense Eq. (2) is incorrect for representing the continuous transformation kinetics, when the law of additivity itself is violated due to the possible non-isokinetic character of the transformation concerned [31]. Such a situation could arise due to changing nucleation, growth or impingement conditions as the transformation gradually progresses towards completion. As an alternative to the combination of isothermal KJMA plus additivity rule, one may adopt the approach followed by Mittemeijer and his group in their study of solid state transformation kinetics by thermal analysis methods [21]. Here, the reaction rate is taken to be a function solely of a path variable that implicitly expresses the thermal history of the sample during the course of transformation. It has been shown that a formal Kolmogorov–Johnson–Mehl–Avrami (KJMA) type integral expression for the fraction transformed X(T), can be derived for practical applications under certain restrictions placed on the type of nucleation, growth and impingement process [21,32]. Under such simplified conditions,

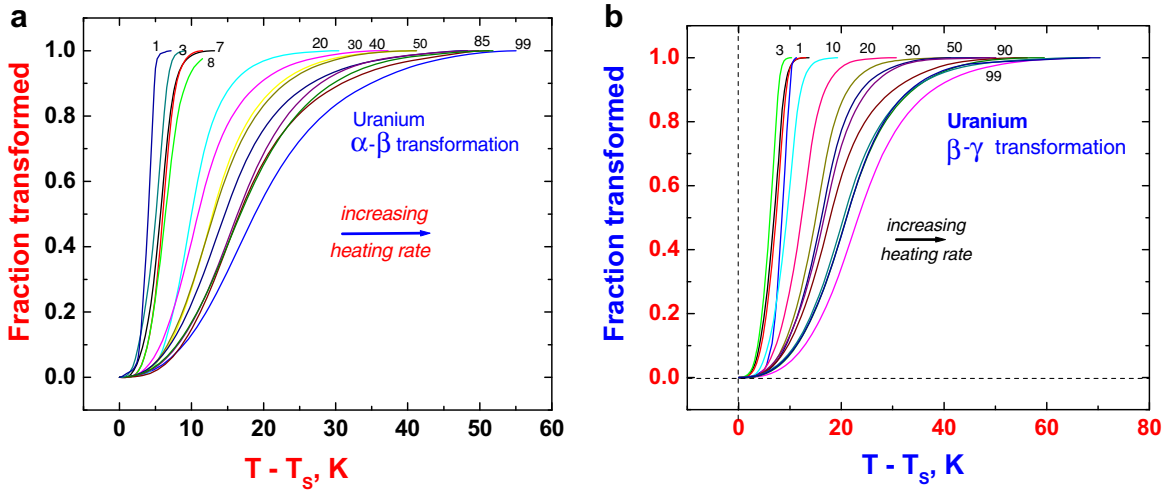

Fig. 6. (a) The transformation plot for the α → β transformation during heating. (b) The transformation plot for the β → γ transformation during heating.

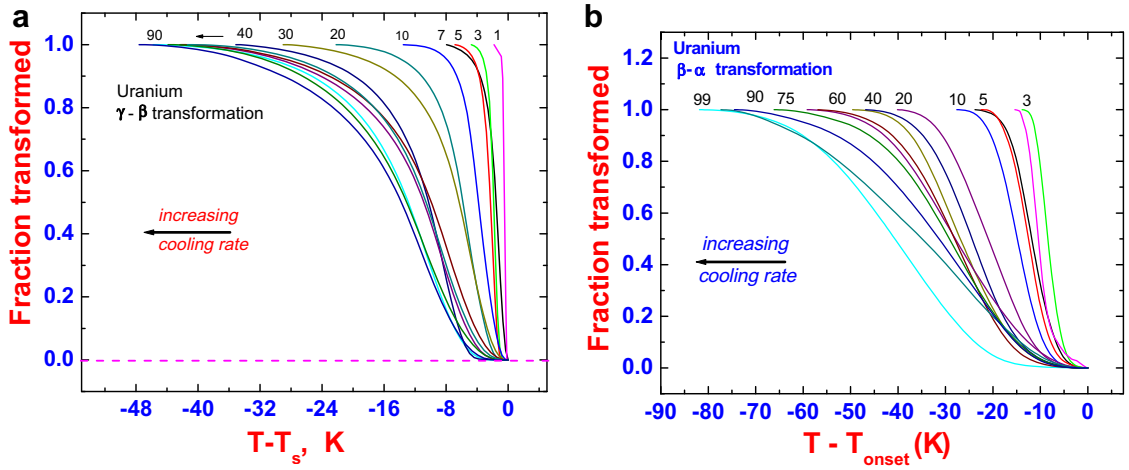

Fig. 7. (a) The transformation plot for the γ → β transformation during cooling. (b) The transformation plot for the β → α transformation during cooling.

Q_{eff} can be identified with a physically based model of nucleation and growth [32]; in fact, it can be shown that Q_{eff} is actually a weighted sum of individual activation energies involved in nucleation and growth processes [32]. In any case, the kinetic parameters of a true rate equation are a function of both X and T and the adoption of a separable rate expression like Eq. (2), is essentially a crude approximation to the real non-linear state of affairs [33]. With this understanding, we adopt in this paper a relatively simple non-isothermal form of KJMA expression for fitting the transformation data of nucleation and growth phenomenon. But, we hasten to add that this is mainly done in an empirical sense to get a consistent analytical description of transformation kinetics. A detailed analysis invoking a microstructural descriptor based prescription of transformation kinetics, as for example carried out by Vandermeer [18] is yet to be completed.

In the present study, for the α → β transformation, the following non-isothermal version of the Kolmogorov–Johnson–Mehl–Avrami (KJMA) formalism for the fraction transformed $X(T)$ as a function of temperature at constant heating rate (β) is adopted [21]

$$X(T) = 1 - \exp\{-k^n[R(T-T_s)^2/\beta Q_{eff}]^n\}. \quad (4)$$

The above expression assumes site saturation type of nucleation. It may be noted that in the above model, we have chosen T–T_S, the temperature increment with respect to the experimentally observed threshold or onset temperature (T_S) as the independent variable, since this corrects in an apparent manner for the error

Table 4
Listing of the kinetics parameters estimated for the α → β transformation using Eq. (4)

Heating rate (β) (K min^{-1})	Q_{eff} (kJ mol^{-1})	$k_o \times 10^{11}$ (s^{-1})	n	k (s^{-1})	k/β (K^{-1})	R^2 value for the fit
1	180	2.1	2.67	20.5	1231	0.999
3	176	2.2	1.72	35.9	718	0.998
5	174	3.0	2.06	60.4	724	0.997
7	176	4.0	1.73	63.2	541	0.999
10	182	7.3	1.62	57.3	344	0.998
20	186	10.9	1.41	54.6	164	0.994
30	188	14.8	1.05	61.3	123	0.995
40	190	18.6	1.08	59.6	89	0.997
50	191	24.8	1.01	71.1	85	0.997
60	193	30.6	0.93	66.9	67	0.996
75	194	33.3	0.98	72.3	58	0.998
85	195	43.0	0.93	74.6	53	0.994
90	197	50.6	0.93	77.5	52	0.998
99	199	56.3	0.85	62.8	38	0.997

The Q_{eff} values are rounded of to nearest integer, the k and n values to one and two decimal points respectively.

incurred in not accounting precisely for the true start of the transformation corresponding to near zero transformed fraction ($X = 0$). The Arrhenius rate constant k is given by Eq. (3). n is the so-called avrami or transformation exponent, whose theoretical value (ranging from 0.5 to 4) depends on whether the transformation is bulk diffusion or interface controlled, besides the dimensionality of growth. Since, only allotropic transformations are being dealt with here, the transformation kinetics is taken to be interface controlled. The dimensionality of growth may take various values. The experimental $X(T)$ data for both the on–heating transformations, namely the $\alpha \rightarrow \beta$ and $\beta \rightarrow \gamma$ are fitted using Eq. (4) by means of a standard non-linear optimisation routine and the resulting values for the kinetic quantities namely Q_{eff}, k_o, and n are listed in Table 4 for the $\alpha \rightarrow \beta$ phase change. Table 5 presents the same information for $\beta \rightarrow \gamma$ phase change. As may be judged from these tables, the value of n for the overall transformation kinetics exhibits a gradual decrease with increasing heating rate, suggesting thereby the changing role of nucleation and growth characteristics with the extent of transformation. The apparent overall activation energy Q_{eff} shows a mild increase with respect to β. Putting it more candidly, the ratio k/β, representing the heating rate normalised value of the rate constant, exhibits a remarkable decrease with increasing heating rate. While the physical implication of this point will be addressed in the discussion section, it is sufficient to note here that not withstanding the theoretical restrictions placed on its applicability, a simplified KJMA model is able to provide a good analytical fit for both $\alpha \rightarrow \beta$ and $\beta \rightarrow \gamma$ transformation kinetics.

3.4. Transformation kinetics upon cooling

An attempt to fit the $X(T)$ data for the $\gamma \rightarrow \beta$ transformation on cooling by means of Eq. (4) turned out to be unsuccessful. This is in a sense expected, since this reverse transformation on cooling is known to be martensitic in character [8]. Further, the transformation plots obtained in the present study are also non-sigmoidal in character (see, Fig. 7(a)) suggesting thereby the inapplicability of the standard KJMA formalism for modelling the displacive transformation kinetics. In view of this, we have invoked the following empirical expression given in Eq. (5) for fitting the temperature dependent progression of the $\gamma \rightarrow \beta$ martensitic transformation

$$X(T) = \exp\{-[(b'/\beta)(T_s - T)]^n\}. \quad (5)$$

In the above expression, β is the cooling rate in K s^{-1}, T_s is the onset temperature in Kelvin and n is a constant. By setting $(b'/\beta)^n = b$, a simple two-parameter description of $\gamma \rightarrow \beta$ transformation after the well-known empirical framework of Koistinen and Marburger (K–M) is readily obtained [34]. It must be added that in the original K–M prescription, n is taken to be unity [34]; but we allowed it to vary here in order to get better numerical agreement. The results of fitting of the present experimental data using Eq. (5) are tabulated in Table 6. It is useful to note that just as in the case of $\alpha \rightarrow \beta$ and $\beta \rightarrow \gamma$ transformations wherein, the value of k/β changed with β, the values for b' also exhibited an increase with increasing cooling rate (Table 5). Since Eq. (5) is empirical in origin, it is not possible to provide a physicochemical basis for the cooling rate variation of parameter b. The negative value of n arises from the fact that with positive values for the argument $(T_s–T)$, the transformation extent $X(T)$ increases with decreasing temperature.

In a similar manner, the transformation data $X(T)$ for the $\beta \rightarrow \alpha$ transformation during cooling have also been modelled by the following empirical expression proposed by Kamamoto [35],

$$X(T) = 1 - \exp\{-[b'/\beta \times \tau]^n\}. \quad (6)$$

where $\tau = (T_s–T)/(T_s–T_f)$, is a dimensionless quantity defined in terms of T_s and T_f. b and n are empirical fit-constants. Again by setting $(b'/\beta)^n = b$, we obtain a simple two-parameter model for the variation of transformation extent with temperature. As a passing remark, we may also add that the empirical expression of Kamamoto is not known to have been used for describing displacive transformation kinetics, since it is basically a recasting of a KJMA nucleation and growth type kinetics [36]; but with the major advantage that it provides a better numerical description of certain complicated nucleation and growth kinetics, but with poor interpretability of the fit parameters in terms of a rigorous physical model. Kamamoto's expression is more generic of diffusional

Table 5
Listing of the kinetics parameters estimated for the $\beta \rightarrow \gamma$ transformation using Eq. (4)

Heating rate (β) (K min^{-1})	Q_{eff} (kJ mol^{-1})	$k_o \times 10^{11}$ (s^{-1})	n	k (s^{-1})	k/β (K^{-1})	R^2 value for the fit
1	159	2.50	3.29	4.0	242.5	0.999
3	147	3.50	2.07	20.4	407.7	0.999
5	143	2.50	2.03	23.6	283.4	0.999
7	143	3.70	1.91	36.5	312.5	0.999
10	144	3.20	1.97	28.5	171.2	0.999
20	151	7.60	1.70	33.3	99.8	0.999
30	154	10.30	1.56	32.8	65.7	0.999
40	155	12.40	1.42	36.7	55.1	0.999
50	155	14.30	1.33	42.5	51.0	0.999
60	157	18.20	1.14	40.4	40.4	0.996
75	164	34.70	1.16	38.7	30.9	0.998
85	165	48.10	1.14	45.9	32.4	0.997
90	166	52.90	1.18	47.9	31.9	0.998
99	175	128.70	1.14	41.4	25.1	0.997

The Q values are rounded of to nearest integer, the k and n values to one and two decimal points respectively.

Table 6
Listing of the kinetics parameters obtained by fitting the observed $\gamma \rightarrow \beta$ transformation data to Eq. (5)

Cooling rate (β) (K min^{-1})	b' (s^{-1})	n	R^2 value for the fit
1	0.047	−3.28	0.999
3	0.030	−4.14	0.997
5	0.042	−3.40	0.998
7	0.097	−1.97	0.992
10	0.052	−2.67	0.989
20	0.069	−2.58	0.994
30	0.099	−2.05	0.993
40	0.075	−2.81	0.999
50	0.093	−2.22	0.995
60	0.126	−2.04	0.992
75	0.117	−2.34	0.991
85	0.163	−2.28	0.993
90	0.131	−2.33	0.993
99	0.152	−2.55	0.995

Table 7
Listing of the kinetics parameters obtained by fitting the observed $\beta \rightarrow \alpha$ transformation data to Eq. (6)

Cooling rate (K min^{-1})	b' (K s^{-1})	n	R^2 value for the fit
1	0.025	5.36	0.999
3	0.078	4.36	0.998
5	0.138	3.89	0.999
7	0.216	3.43	0.999
10	0.286	3.89	0.999
20	0.573	3.13	0.997
30	0.847	3.48	0.997
40	1.16	3.46	0.997
50	1.57	2.61	0.998
60	1.82	3.29	0.998
75	2.49	2.70	0.999
85	2.66	2.13	0.996
90	3.05	2.36	0.999
99	2.96	3.20	0.998

transformation kinetics. It should be mentioned here that neither the simplified KJMA Eq. (4) nor the K–M expression Eq. (5) were able to fit satisfactorily the observed $X(T)$ data of $\beta \rightarrow \alpha$ transformation, partly because, this transformation is known to adopt a mixed mode depending upon the cooling rate, as Burke and Dixon have argued long ago [16]. In Table 7, the parameters, b and n obtained by fitting the experimental results to Eq. (6) are listed.

4. Discussion

4.1. Nucleation modes and the role of heating rate

The present study clearly brought out the fact that the transformation arrest temperatures for all the allotropic phase changes are found to be strongly dependent on the heating or cooling rate, a fact, which is inherent to many nucleation and growth processes and for which quite a few explanations have also been proposed based on established viewpoints on nucleation and growth processes [37]. In the case of uranium, such a finding had been recorded earlier as well; however, to the best of our knowledge a careful reasoning of the underlying physical phenomenon in terms of appropriate metallurgical factors has not been undertaken so far. The present investigation conducted with nearly thermal gradient free small samples, although in a restricted range of (10^0–10^2 K min^{-1}) heating and cooling rates, clearly suggests that in case of the $\alpha \rightarrow \beta$ transformation, a split DSC peak profile or a peak with shoulder is observed for slower heating rates, while a standard, single peak is observed for faster rates of heating.

At this point it is rather instructive to recall the fact that very similar observations have recently been recorded by Liu et al. in their thermal analysis characterisation of the kinetics of γ (fcc) $\rightarrow \alpha$ (bcc) phase change during cooling in fairly large grained pure iron samples [38]. A direct comparison of our result with the findings of Liu et al. suggests that there could be a possible change in the transformation nucleation mechanism, when the starting grain size exceeds a threshold limit. A so-called abnormal mode of allotropic phase change is advocated for fairly large starting grain size samples. Stated briefly, the explanation given by Liu, Sommer and Mittemeijer [38] rests on the fact that repeated autocatalytic nucleation of the product phase ahead of the moving transformation front is what is responsible for the occurrence of a split or multiple peak phenomenon in DTA peak profiles. But what is important to note is that such '*ahead of the interface bulk nucleation events*', must occur in discrete pulses with passage of time to account for the multi-peaked nature of the variation of the transformation rate with time. In what follows, we seek a logical exploration of such a possibility for a simple nucleation growth mediated phase transformation phenomenon.

Taking the general case of a phase transformation involving no change in composition and occurring upon heating for example, it can be argued, that for a given initial microstructure and heating rate, owing to the ubiquitous presence of energy barriers associated with diverse modes of nucleation, appreciable overheating of the sample results before product phase nucleation can be effected. This extent of superheating, or more appropriately the degree to which the transformation onset temperature is made to exceed its equilibrium value is a function of the heating rate. If τ, is the typical incubation time for steady state nucleation of β phase at temperatures that are not too removed from the equilibrium transformation point (T_o), then for a sample that is heated at a rate of β, the first instances of nucleation would be registered at a temperature, $T(\beta)$ that is given to a first approximation as

$$T_s(\beta) = T_o + \beta\tau. \tag{7}$$

In the present study, the variation of $T(\beta)$ with β is rather non-linear (Fig. 4), which in essence suggests that our simple reasoning, albeit technically correct is quantitatively inadequate, in the sense, that when more than one type of nucleation modes with different characteristic time scales, $\tau_{\cdot 1}$ and $\tau_{\cdot 2}$ are under operation, then the linear approximation given in Eq. (7) needs to be 8 modified accordingly. In the present case, we chose the following form

$$T_n(\beta) = T_o + \beta(f_1\tau_{\cdot 1} + f_2\tau_{\cdot 2} + \cdots). \tag{8}$$

In the above relation, we have further included two additional weighting factors, f_1 and f_2 that reflect the relative contributions from the two different nucleation modes to overall number density of nuclei. Further, if we make these weighting factors sensitive to the variations in heating rate (β), that is $f_1 = f_1(\beta)$ and $f_2 = f_2(\beta)$, then a non-linear variation of the transformation arrest temperatures with β is readily obtained.

Recasting this model in terms of the standard output of a DSC experiment, namely the total rate of transformation, $(dX/dt)_\beta = (dX/dT)_\beta \times \beta$, we obtain

$$(dX/dT)_\beta = (1/\beta)\{f(X_1) \times k_1(T) + f(X_2) \times k_2(T)\}. \tag{9}$$

The above relation is written using the simple separable representation of $(dX/dT)_\beta$ invoked in Eq. (2). $k_1(T)$ and $k_2(T)$ are respective Arrhenius rate constants. Thus it emerges from this reasoning that the occurrence of a composite peak structure with split or multiple shoulders is due to the operation of *concurrent*, yet *differently weighted* contributions from two different reaction mechanisms, which could in principle be multiple and concurrent nucleation modes, or growth mechanisms or a combination of these two.

For a sample with a fairly large starting α phase grain size, the choice of small heating rates (1–10 K min^{-1} in our experiment) with resulting small overheating (T_s–T_o), would first enable the heterogeneous nucleation of the β phase from triple junctions, that is grain corners, then grain edges and finally in the grain interior. The incidence of a large starting grain size results in a net reduction in the number of potential low energy nucleation sites (grain edges and corners) to start with. Hence, after the quick initial exhaustion of such low activation energy nucleation sites, there is a drop in the nucleation rate from this mode. In addition, the formation of β with a larger specific volume and elastic stiffness than the parent α-grain will result in the development of stresses at the transformation interface and this would also effectively reduce the driving force available for further propagation of the transformation. This then results in a slowing down of the reaction rate that would reflect as a dip or a kink in the corresponding DSC profile. This kinetic retardation of nucleation is only temporary in that it will be followed by fresh nucleation events at '*more difficult to nucleate sites*' such as grain interior, which will now become accessible upon reaching to higher temperatures with further passage of time. Thus repeated nucleation events at successively higher time or temperatures in case of continuous heating can in principle lead to multiply peaked DSC profile. Now, if we chose to heat the sample at a faster rate ensuring thereby the attainment of a higher transformation start temperature, then both homogeneous and heterogeneous types of nucleation events are triggered simultaneously and with the predominant contribution coming from homogeneous nucleation mode for larger grain sized samples, a normal DTA profile with single peak is obtained.

If the starting α phase grain size is very small, then at all points of time, there will be present enough catalytic nucleation sites to ensure the continuous propagation of the transformation front for practically all the heating rates. Thus, there exists a threshold grain size above which only, the anomalous transformation mode is triggered in simple interface controlled nucleation and growth transformations [38].

To complete the explanation, we may also add that at very high rates of cooling (10^6 K s^{-1}), as for example adopted by Duwez [15], it emerges from Eq. (7), that a very large undercooling and hence a significant pile up of the thermodynamic driving force is made available at T_s, for both initiation and progress of the transformation. This higher driving force can facilitate the rapid propagation of the transformation front. Thus, the small number of β phase nuclei that are the first ones to form, say in the matrix α phase triple junctions for reasons of energetics can now transform by rapid advancement of the α/β interface. Although, the present study is not concerned with such very high heating or cooling rates, there are adequate precedence in literature to support the fact that massive and martensitic modes of allotropic transformation do in fact occur for faster rates of heating and cooling [39–41]. An analysis of the present results on the lines of nucleation controlled massive transformation mode is currently underway [42].

4.2. Kinetics parameters: heating rate dependence of Q_{eff}

At the outset, it must be admitted that following the reasoning advocated by Berkenpas et al. with regard to a model based analysis of transformation kinetics [43], and by Sewry and Brown with regard to the intricacies involved in a so-called model-free reaction kinetics [44], it is not clear as to how far the values extracted for the kinetic quantities by fitting the transformation data to *empirical* rate expressions are meaningful in a fundamental sense. Nevertheless, we indulge in such an exercise in the present study only to offer a plausible estimate of Q_{eff} involved in the structural changes in pure uranium. A straight forward application of Kissinger or Ozawa formalism [45] for effective linearisation of the data on shift in the peak transformation temperature with heating rate yielded non-linear plots that in spirit obviates the applicability of these methods for extracting the kinetics quantities. In fact, a similar observation had earlier been recorded in case of a DTA study on the allotropic transformation of plutonium [46]. In deference to the limited scope of this study, we do not present a detailed discussion on this issue, but it suffice to say that the application of Kissinger like method for extracting the apparent activation energy of transformations involving multiple and concurrent steps is strictly not correct [47]. In the present study, this difficulty is however overcome by directly fitting the transformation data to suitable empirical reaction models by means of a robust non-linear optimisation routine.

The values for Q_{eff} thus obtained for the α → β phase change varies from 174 to 199 kJ mol^{-1}, and for the β → γ transformation, it ranges from 143 to 175 kJ mol^{-1} (Tables 4 and 5). The activation energy reported for self-diffusion in the three structural modifications of uranium are about: α-U:167.5, β-U: 175.8 and γ-U: 115.1 kJ mol^{-1} [44]. It must be remarked that we have adopted a simplified version of KJMA model, which do not really incorporate the role of changing nucleation and growth rates with the extent of transformation. Notwithstanding this serious limitation, and taking cognisance of the fact that Q_{eff} is actually a weighted sum of individual contributions from nucleation (Q_N) and growth (Q_G), we may write, $Q_{eff} = pQ_N + qQ_G$, with p and q being arbitrary constants. It is normally the case that Q_N, which is of the order of a few kilo joules per mole is much less than Q_G. Under this condition, we may note that the measured activation energies are primarily reflective of the growth component and going by the fact Q_{eff} is in the same range as the self-diffusion activation energies, we may conclude that α → β and β → γ transformation mechanism is one of involving atomic jumps across the phase interface. As for the n values are concerned, we refrain from attributing a definite physical meaning, as we primarily treat it as a fit parameter in this study. Besides, it must also be added that the kinetic quantities, k_o, Q_{eff} and n form a unique kinetic triplet in the sense that a change in one parameter totally off-sets the overall goodness of fit.

In the present study, we also note a small but steady increase in Q_{eff} with heating rate. This reflects probably the increasing degree of difficulty associated with nucleation at high rates of heating, as growth rates at these temperatures are expected to be high and remain constant. The dramatic role of heating rate on k/β, the *overall* heating rate normalised rate constant is nicely brought out in Fig. 8. Quite interestingly, the observed behaviour for both α → β and β → γ transformations can be fitted to a simple power law of the following form

$$k/\beta = C(\beta)^{-m}. \tag{10}$$

From, Eq. (10) it is possible to define a dimensionless quantity, ξ characterising the bi-logarithmic variation of k with β. Thus, it emerges from Eq. (10)

$$\xi = d\ln k/d\ln\beta = (1-m). \tag{11}$$

The value of m obtained in the present study is 0.99 for α → β and 0.72 for β → γ transformation. The physical import of this finding is that there is present an intrinsic scaling behaviour in the heating

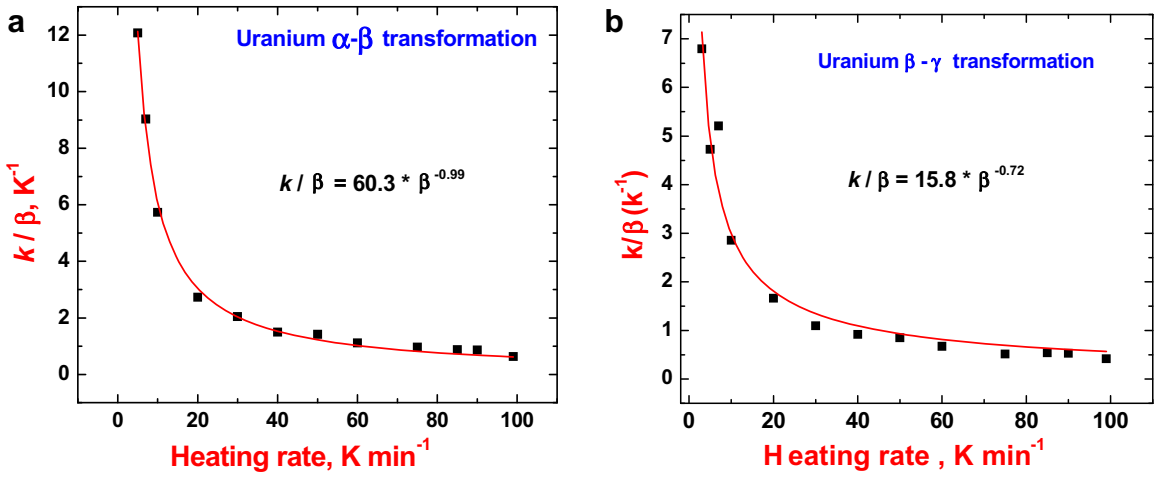

Fig. 8. (a and b) The variation of heating rate normalised Arrhenius rate constant (k/β) with β for (a) α → β and (b) β → γ transformations. The line represents the power law fit to the observed data.

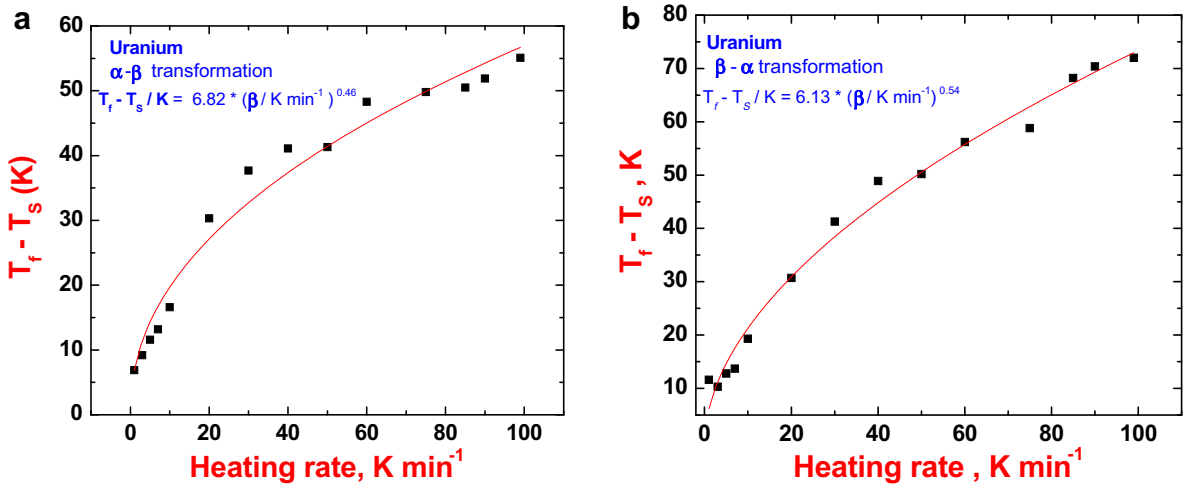

Fig. 9. (a) and (b) The heating rate dependence of the width of the transformation zone (T_f–T_s) for (a) the α → β and (b) β → γ phase transformation. The line in both graphs represents the analytical fit to the experimental data. The nearly same value of the power law exponent for both phase changes is worth noting.

rate dependence of $(dX/dT)_\beta$ for both the on-heating transformations. If we were to assume the validity of standard isoconversional rate equation formalism, namely that given by Eq. (2) and (3), it may be deduced from the scaling law presented in Eq. (11) that for fixed X, the fraction transformed, the pseudo reaction rate $(dX/dT)_\beta$, varies with respect to heating/cooling rate as $(\beta)^{-m}$. Thus, the knowledge of $(dX/dT)_\beta$, for one standard heating rate with attending information on the Arrhenius rate constant can be used to generate the transformation plot for other heating rates. This predictive capability is rather inbuilt in our transformation plots (Fig. 6(a) and (b)) in the sense that the gradually changing nature of the slope of transformation plots with increasing heating rate is readily apparent. If on the other hand, the heating rate has no influence on the transformation kinetics, then the transformation curves for different heating rates, when plotted on a normalised temperature (T–T_S) basis, should all merge to give a single master curve. However, such is not the case witnessed in the present study. Before closing this point, we may also add that this simplified interpretation of scaling law rests on the validity of isoconversional rate equation hypothesis; but in reality this is rather questionable [21]. In deference to the limited scope of our study, this aspect is not dealt with here in any detail.

4.3. Other general aspects

The other additional point that remains to be clarified is with regard to the heating rate dependence of the extent of transformation completion. It is generally known, that many solid state nucleation and growth transformations seldom proceed to 100% completion at faster rates of heating. Accordingly, the total peak area, taken to be proportional to the enthalpy of phase change is a decreasing function of the heating rate. This fact is by and large reflected in the results obtained (Tables 2 and 3). It may be seen that compared to the β → γ phase change, the area for the α → β transformation shows a preponderant decrease with increasing β, while for γ → β martensitic phase change on cooling, the corresponding peak area is fairly a constant, which is consistent with the a thermal character of the transformation.

The other useful point to emerge from this study is that for both α → β and β → γ phase changes, the effective width of the transformation domain represented by the differential temperature, T_f–T_s, varies approximately as the square root of the heating rate. This is illustrated in Fig. 9(a) and (b) for α → β and β → γ phase transformations respectively. It can be seen that very similar exponent values are noticed for both phase changes. At present this aspect has not been fully analysed and understood, but an attempt to arrive at a comparative interpretation of this finding in terms of a similar finding in massive phase transformations suggests that the heating rate dependence of the nucleation event could be one of the reasons [48,49]. Considering the experimental uncertainties involved, the values of the power law exponents obtained from the fits shown in Fig. 9 may be taken as close to 0.5, a fact supported by the findings of Bhattacharya et al. [48] and also by Caretti and Bettorello [49] regarding nucleation controlled massive mode of phase change. Admittedly a mathematical treatment on this line is not carried out in this study, as reliable values for many parameters like interface energy, mobility *etc*., are currently lacking for uranium. But further research on evolving a physically based description of transformation data on the lines of Vandermeer's approach [18] is currently under way [42].

5. Conclusions

(i) A comprehensive thermal analysis investigation of the kinetics of allotropic phase changes in uranium metal has been undertaken.

(ii) The transformation temperatures exhibit a strong non-linear variation with the heating or cooling rate. For small heating rates, the DSC profile for the α → β transformation contains a shoulder, which feature is however absent for larger heating rates. For small heating rates, the relative competition between heterogeneous and homogeneous grain interior nucleation events control the structure development.

(iii) The kinetics of both the on-heating phase changes, namely, α → β and β → γ are described well by a standard KJMA formalism for the nucleation and growth process. This however is not true for the β → α and γ → β phase changes that occur during cooling.

(iv) The effective activation energies estimated for the on-heating phase transformations are of the same order of the activation energies involved in the self-diffusion process in α and β uranium lattices.

(v) The kinetics of γ → β phase change is found to be non-sigmoidal in character and is well described by the empirical Koistinen and Marburger expression for the martensitic transformations. The β → α phase change on the other hand is sensitive to cooling rate and is accounted for by the empirical Kamamoto's relation for the fraction transformed.

(vi) The heating or cooling rate normalised empirical rate constant, namely k/β exhibits a power law relationship with β.

Acknowledgements

The authors sincerely acknowledge the anonymous reviewer, whose comments have served to enhance the clarity and content of our work. Mrs Mythili helped in getting the SEM–EDX analysis. Mrs. Josephine Prabha is thanked for many stimulating discussions in the course of this work. The authors are also grateful to Dr M. Vijayalakshmi, Dr K.B.S. Rao, Dr P.R. Vasudeva Rao and Dr Baldev Raj, for their sustained support and encouragement.

References

[1] A.N. Holden, Physical Metallurgy of Uranium, Addison-Wesley Publishing Company, Reading, MA, 1958.
[2] B. Blumenthal, J. Nucl. Mater. 2 (1960) 23.
[3] S.E. Moore, K.K. Kelley, J. Am. Chem. Soc. 69 (1947) 2105.
[4] D.C. Ginnings, R.J. Corruccini, J. Res. Natl. Bur. Std. 39 (1947) 309.
[5] A.I. Dahl, M.S. Van Dusen, J. Res. Natl. Bur. Std. 39 (1947) 53.
[6] P. Gordon, A.R. Kaufman, Trans. A.I.M.E. 188 (1950) 182.
[7] H. Okamoto, J. Phase Eq. 13 (1992) 109.
[8] D. Blake, R.F. Hehemann, Transformations in uranium base alloys, in: J.J. Burke, D.A. Colling, A.E. Gorum, Jacob Greenspan (Eds.), Physical Metallurgy of Uranium Alloys, Brook Hill Publishing Company, MA, 1976, pp. 189–218.
[9] K.M. Pickwick, W.J. Kitchingman, J. Nucl. Mater. 19 (1966) 109.
[10] R.D. Townsend, J. Burke, J. Nucl. Mater. 17 (1965) 279.
[11] I.F. Barwood, B.R. Butcher, J. Nucl. Mater. 8 (1963) 232.
[12] W.J. Kitchingman, K.M. Pickwick, I.G. Brown, R.J. Edwards, J. Nucl. Mater. 18 (1966) 219.
[13] G. Donze, J. Nucl. Mater. 5 (1962) 150.
[14] J.J. Rechtein, R.D. Nelson, Metall. Trans. 4b (1973) 2755.
[15] P. Duwez, J. Appl. Phys. 24 (1953) 152.
[16] J. Burke, P.H. Dixon, J. Nucl. Mater. 7 (1962) 38.
[17] H. Yakel, A review of X-ray diffraction studies in uranium alloys, in: J.J. Burke, D.A. Colling, A.E. Gorum, Jacob Greenspan (Eds.), Physical Metallurgy of Uranium alloys, Brook Hill Publishing Company, MA, 1976, pp. 259–308.
[18] R.A. Vandermeer, Metall. Trans. 17A (1986) 1717.
[19] D. Turnbull, Trans. AMIE 191 (1951) 661.
[20] Y.C. Liu, F. Sommer, E.J. Mittemeijer, Acta Mater. 54 (2006) 3383.
[21] F. Liu, F. Sommer, E.J. Mittemeijer, Int. Mater. Rev. 52 (2007) 193.
[22] J. Sietsma, S. van der Zwaag, Acta Mater. 52 (2004) 4143.
[23] R.G. Thiessen, I.M. Richardson, J. Sietsma, Mater. Sci. Eng. A 247 (2006) 223.
[24] P.R. Rios, Acta Mater. 53 (2005) 4893.
[25] M.J. Richardson, in: K.D. Maglic, A. Cezairliyan, V.E. Peletsky (Eds.), Compendium of Thermophysical Property Measurement Techniques, vol. 2, Plenum Press, New York, 1992, p. 519.
[26] J.A. Martins, J.J.C. Cruz-Pinta, Thermochim. Acta 332 (1995) 179.
[27] E. Gmelin, S.M. Sarge, Thermochim. Acta 347 (2000) 9.
[28] A.T.W. Kempen, F. Sommer, E.J. Mittemeijer, Thermochim. Acta 383 (2002) 23.
[29] M.J. Starink, Thermochim. Acta 404 (2003) 163.
[30] P. Kruger, J. Phys. Chem. Solids 54 (1993) 1549.
[31] C. Verdi, A. Visintin, Acta Metall. 35 (1982) 2711.
[32] G. Ruitenberg, E. Woldt, A.K. Petford-Long, Thermochim. Acta 378 (2001) 97.
[33] M.T. Todinov, Acta Mater. 44 (1996) 4697.
[34] D.P. Koistinen, R.E. Marburger, Acta Metall. 7 (1959) 59.
[35] S. Kamamoto, T. Nishimori, S. Kinoshita, Mater. Sci. Tech. 1 (1985) 798.
[36] I.I. Boyadjiev, P.F. Thompson, Y.C. Lam, ISIJ Int. 36 (1996) 1413.
[37] Y. Zhu, J. Devletian, J. Mater. Sci. 26 (1991) 6218.
[38] Y.C. Liu, F. Sommer, E.J. Mittemeijer, Philos. Mag. 18 (2004) 1853.
[39] C.A. Apple, G. Krauss, Acta Metall. 20 (1972) 849.
[40] W.J. Kaluba, R. Taillard, J. Foct, Acta Mater. 46 (1998) 5917.
[41] E.A. Wilson, ISIJ Int. 34 (1994) 615.
[42] A.K. Rai, Unpublished Research, 2008.
[43] M.B. Berkenpas, J.A. Barnard, R.V. Ramanujan, H.I. Aaronson, Scr. Metall. 20 (1986) 323.
[44] J.D. Sewry, M.E. Brown, Thermochim. Acta 390 (2002) 217.
[45] M.J. Starink, Int. Mater. Rev. 40 (2004) 191.
[46] R.D. Nelson, J.C. Shyne, J. Nucl. Mater. 19 (1966) 345.
[47] S. Raju, Unpublished Research, 2008.
[48] S.K. Bhattacharyya, J.H. Perepezko, T.B. Massalski, Acta Metall. 22 (1974) 879.
[49] J.C. Caretti, H.R. Bettorello, Acta Metall. 31 (1983) 325.